

Black bear colour polymorphism through a fragmented Snell's window

THOMAS E. REIMCHEN*, DANIAL HUNTER and JAKOB H. EGGENBERGER

Department of Biology, University of Victoria, PO Box 1700, Victoria, B.C., V8W 2Y2, Canada

Received 30 January 2021; revised 21 April 2021; accepted for publication 26 April 2021

The white colour morph of the black bear (*Ursus americanus kermodei*) occurring on islands on the coast of British Columbia, western Canada, captures more salmon (*Oncorhynchus* spp.) than does the black morph and is hypothesized to have reduced contrast against the sky from the visual perspective of the salmon. We tested this hypothesis in a natural salmon stream by recording the number and proximity of chum salmon (*Oncorhynchus keta*) approaches ($N = 1617$ fish, 91 trials) towards life-size bear models differing in body and leg coloration under a mixed forest-sky canopy. Although salmon approached the white models at a much higher rate than black models, consistent with camouflage, we found greater abrupt evasions to the black models, largely independent of their contrast against the above-surface or below-surface backgrounds. Upward-facing sub-surface video-imaging through the rippled water-air interface indicated major visual fragmentation of the model's integrity. We suggest that increased evasiveness to black models reflects an evolutionary response due to 3+ million years of trophic interaction between salmon and bears, and that the major differences between calm vs. rippled conditions through the optical cone (Snell's window) at the water-air interface remains a largely unexplored theme in assessing foraging preferences and adaptive coloration within and among species using the water-air interface.

ADDITIONAL KEYWORDS: camouflage – experimental models – field experiment – Kermode bear – salmon – Snell's window – spirit bear – visual contrast – water-air interface.

INTRODUCTION

One of the most conspicuous pelage colour polymorphisms in a large terrestrial carnivore occurs in the American black bear (*Ursus americanus kermodei*) in coastal British Columbia where on several remote islands, a highly visible white morph (Kermode bear) can reach 10–30% of the population (Cowan & Guiguet, 1956; Fig. 1A). The white pelage originates from a mutation at the melanocortin gene, segregates as Mendelian recessive and is not expressed in the heterozygote (Ritland *et al.*, 2001). That the white morph is rarely found on the mainland clearly argues for the importance of geographical isolation in the persistence of this polymorphism on the coastal islands (Marshall & Ritland, 2002; Hedrick & Ritland, 2011). Heterozygote advantage, a plausible mechanism for the maintenance of polymorphism (Ford, 1964), does not contribute to the persistence of this colour polymorphism since heterozygotes are

not excess to predicted frequencies based on Hardy–Weinberg frequencies (Hedrick & Ritland, 2011; Service *et al.*, 2020). Migration from the adjacent mainland would not facilitate an equilibrium since more than 99% of the potential migrants would be black morphs; this should have resulted in the loss of the less common white allele, which is not the case. The polymorphism is not transient since oral history of the First Nations indicates long-term persistence of the white bear (Service *et al.*, 2020). Although the Kermode subspecies has an approximate 360 000-year divergence from other continental subspecies, it is closely related to the endemic bears on the adjacent Haida Gwaii archipelago and on Vancouver Island, neither of which have the white morph (Byun *et al.*, 1997). These multiple studies cumulatively suggest that the long-term persistence of the white bear cannot be simply a function of isolation but is the result of some long-term fitness advantage over the black morph.

One of these advantages is foraging ability. Field studies have shown that these coastal bears capture spawning pink salmon (*Oncorhynchus gorbuscha*)

*Corresponding author. E-mail: reimchen@uvic.ca

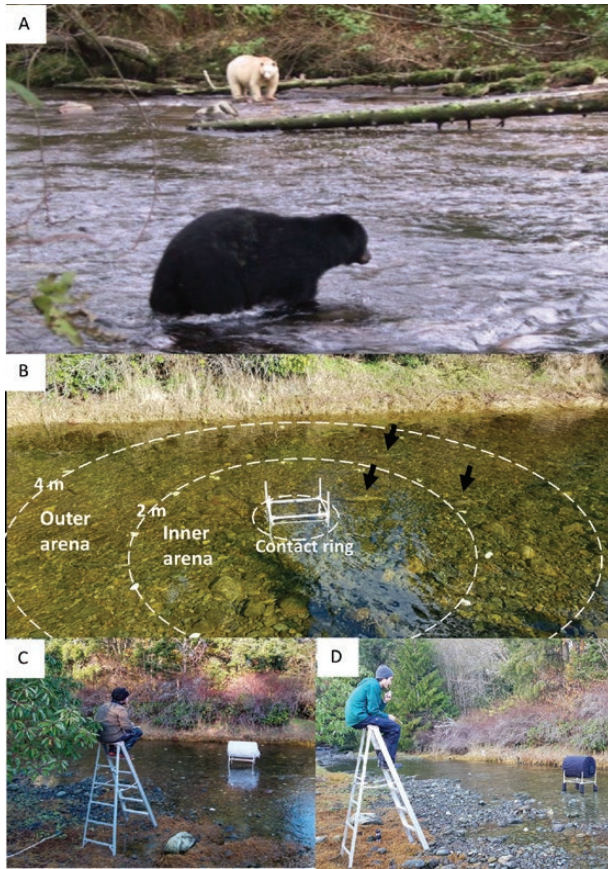


Figure 1. Methodology. A, white and black morphs at Riordin Creek, Gribbell Island, British Columbia. A, Study area at Ayum Creek, Vancouver Island, British Columbia with model frame with white pebbles positioned every 30° around the perimeter of 2 m and 4 m rings. Dashed white lines are virtual to show the edges of the arenas. Black arrows indicate migrating chum salmon. Stream flow is from left to right. C, observation platform showing model configuration with white body and no legs (WO). D, observation platform showing model configuration with black body and black legs (BB).

during darkness, twilight and daylight (Klinka & Reimchen, 2009a). Relative to the black morph, the white morph has marginally reduced capture rates of salmon during darkness but increased capture rates during daylight (Klinka & Reimchen, 2009b) and overall, has greater consumption of salmon based on stable isotope analyses of hair shafts (Reimchen & Klinka, 2017). Exposure of spawning salmon to an in-stream standing human with alternate ‘coat colours’ indicated significantly less avoidance to the white model relative to the black model during daylight but not during darkness. The authors hypothesized that the higher salmon capture success of the white morph was associated with their reduced detection against the light background of the sky (Klinka & Reimchen, 2009b; Supporting Information, Video S1).

In the present study, we test this hypothesis and examine several additional factors not considered in the original field study (Klinka & Reimchen, 2009b). The extent to which salmon respond to a white-coated or black-coated human standing in a shallow stream may not be applicable to their responses to the low profile of a bear. For a fish in a stream with a flat surface, the entire above-surface skyscape/landscape is refracted into a 97° optical cone (Snell’s window) with the sky dominating the central parts of the cone and the horizon or shoreline projecting into the edge of the cone (Horváth & Varjú, 1995). Detection of a predator standing on shore will be dependent on how high it projects onto the cone and the contrast against the sky or terrestrial background. However, under a wave or rippled surface, Snell’s window expands in breadth and can reach 180° but with major fragmentation of the above-surface skyscape/landscape (Lynch, 2015). This could limit resolution or identification of any shape in the fragmented window. Despite the diversity of predator and prey that interact through the water-air interface and the prevalence of this globally common habitat, it has received very limited attention with respect to animal foraging [with the recent exception of Day *et al.* (2016)]. An additional factor in the original study by Klinka & Reimchen (2009b) is that they did not evaluate the sub-surface (leg) effects, yet one would expect that visual detection of sub-surface shapes would be equally important as those above-surface.

In a natural salmon stream outside the distribution of the Kermode bear, we placed life-sized bear models and monitored the approaches and evasions of spawning chum salmon (*Oncorhynchus keta*). We quantified spectral contrast of the models against sky and forest backgrounds viewed from the perspective of salmon through Snell’s window under flat water and wave-influenced water surfaces. We also examined salmon responses to sub-surface components of the models (leg colour) independent of their body coloration. The horizontal backgrounds against which sub-surface objects are viewed is dark relative to the background of downwelling-light and as such will contrast less than light-coloured objects (Lythgoe, 1979). We predicted fewer avoidance responses of salmon to the above-surface white model when viewed against the sky through Snell’s window, but increased avoidance to sub-surface white legs when viewed against the dark backgrounds.

MATERIAL AND METHODS

We conducted field experiments from 6 to 19 November 2018, during the chum salmon (*O. keta*) spawning run at Ayum Creek on the south end of

Vancouver Island, British Columbia (48°23'29"N, 123°39'36"W). Black bears occur on this stream as well as on the majority of salmon streams in British Columbia; however, the locality is about 500 km from the most southerly distribution of the Kermode bear (Cowan & Guiguet, 1956). The experiments occurred within 100 m of the estuary where the channel is 8 m wide and up to 0.5 m deep. Riparian vegetation is composed of conifers (~ 20 m height) with an approximate 25° open canopy upstream from the testing area and low shrubs (3 m height) and a 120° open canopy downstream. Salmon spawning escapement records, which extend back to 1947, vary from 100 to 3500 chum salmon among years.

A bear-like model was constructed using a welded aluminum frame, a polyvinyl chloride (PVC) barrel (187 L) as a 'body' that rested on top of the frame and PVC tubes (10 cm diameter) as 'legs' that were sleeved over the legs of the frame. We covered the barrel and tubes, which were removable, with opaque black or white polyester fleece cloth to approximate the general visual appearance of black or white bear. Visual sensitivity of migrating adult salmon are broader than human vision [Beaudet *et al.* (1997); see review in Carleton *et al.* (2020)] and as such, the black or white fleece cloth might not be equivalent to what appears to us a black or white bear. Spectral scans (300 to 800 nm) of the cloth using a spectroradiometer (Ocean Optics Inc, SD2000) under overcast natural lighting conditions showed the expected reflectance curves for a black or white surface with low reflectance across all wavelengths for the black cloth. Reflectance off the white cloth paralleled the spectra of atmospheric downwelling light (Hailman, 1977). In initial trial runs in the stream, it was evident that the salmon were responding to the models in a comparable manner (reaction distance, evasive responses) to how they responded to actual bears (Klinka & Reimchen, 2009a) as well as to human in-stream observers with black or white cloaks (Klinka & Reimchen, 2009b). We assume that our current stream study is also a meaningful assessment of salmon responses to black or white coated models.

We used seven different configurations on the model: (1) the control (the frame) with no body-no legs (OO), (2) no body-black legs (OB); (3) no body-white legs (OW); (4) black body-no legs (BO); (5) white body-no legs (WO); (6) black body-black legs (BB) and (7) white body-white legs (WW). As an additional control, we also recorded the number of salmon using the area when no frame was present.

To score the position of migrating salmon relative to the model, we established three concentric arenas around the model: one directly under the model, a second ring 2 m from the model and a third ring 4 m from the model (Fig. 1B). To visualize each ring, we used stream pebbles that were painted white (Krylon Dual Superbond white satin) and positioned every 30°

around the ring. The outer ring spanned the full stream diameter. For each observational trial, we walked to the centre of the stream, causing the salmon to leave the arenas, and placed the model in the central arena, returning immediately to the shore for observations which lasted 12 min for each trial and which were made from a 2 m high step ladder (Fig. 1C-D). Within several seconds, salmon returned to the region of the stream and we recorded their numbers and length of time spent in each arena. In some instances, salmon showed an 'abrupt' evasive response, changing their direction and/or their speed with proximity to the model. We scored this abrupt response for each of the three arenas. Trials were conducted between 08:30 and 14:30 h, the exact timing dependent on the tidal cycle. On sequential trials, we examined opposite treatments (e.g. BO and WO, OB and OW, etc.) to ensure that trials were applied in similar conditions (e.g. cloud cover, number of salmon present, light levels, etc.). Time between trials was approximately 2 to 3 min. In all trials, the 'body' of the model was above and the 'legs' below the water surface.

Using digital image analyses, we estimated the extent of spectral contrast of the bear models against above-surface and below-surface backgrounds through Snell's window. To assess the contrast through a flat surface, we made images at a small lake and for current-induced wave surface, we made images directly at Ayum Creek. We set the bear models in shallow water against a shoreline background dominated by either sky ("light") or forest ("dark") and captured video images with an underwater camera set to a 1920 × 1080 pixel resolution and 30 frames per second. The camera was positioned 0.75 m below the surface tilted upwards at 45° towards the models that were either 2 m or 4 m from the camera. We obtained 30 s of video for each configuration including a reference sequence of the frame (no body). We selected ten images by isolating the most stable continuous 10 s clip from each of the 30 s videos. From these ten segments, we saved an image every 30 frames. To control for changes in ambient light conditions among the trials, we cropped an image of the white body and overlaid this image onto the black body images to remove any differences in lighting conditions between treatments. We converted all of the images to greyscale, including the reference images and quantified for each image the contrast-to-noise ratio ("CNR") where:

$$\text{CNR} = ((\bar{x}_s - \bar{x}_n) / \text{sd}_n)$$

where " \bar{x}_s " is the mean of the greyscale signal image, " \bar{x}_n " is the mean of the greyscale reference image, and " sd_n " is the standard deviation of the greyscale reference image. This index defines the amount of cumulative difference for all pixels in the targeted frame relative to the reference frame.

We captured additional images from the stream channel for legs (sub-surface) and body (above-surface) models. The camera was placed in the middle of the

stream at approximately 15 cm depth and fixed images of the leg colour morphs were obtained at distances of 1 m, 2 m, 3 m and 4 m. For each image, we computed the CNR for the leg relative to an immediate adjacent area of the background spectra (see Fig. 5). For imaging the body through Snell's window, we positioned the models in two regions of the stream, a lower section where there was limited shoreline vegetation and consequently increased background of sky and an upper section with an approximate 65% forest canopy cover over the stream. In each section, we took approximately 5 s of video with the camera positioned at 2 m and 4 m distances (30 cm depth, angled upwards at $\sim 45^\circ$) directed upstream or downstream for each model colour, resulting in 16 model-background conditions. For each of the videos, we captured an average of 45 stop frames (range 35–61) for spectral analyses. Each frame was converted to a greyscale image and we calculated the spatial autocorrelation coefficient for each pixel in the frame using 'autocorr2d' (Ursell, 2020) from which we then derived a mean coefficient for each frame. This coefficient ranges from -1 to 1, where -1 represents perfect negative autocorrelation (i.e. adjacent pixels have opposite brightness values) and where 1 represents a perfect positive correlation (i.e. adjacent pixels have the same brightness value). The mean and median coefficients for each image were calculated and used to assess the extent of background contrast or matching. As an example, a black model against a dark background would have a higher coefficient than a black model against a light background. Among the 16 spectral backgrounds visualized through Snell's window, we would anticipate that the brightest background (lower stream section) would yield lower coefficients for the black model whereas in the darkest background in the upper forested section, the white model would have lower coefficients. Because of the image quality (160 000 pixels), average coefficients per frame ranged over three orders of magnitude among frames but were on average very small ($e-15$).

STATISTICS

A general linear model ("GLM") was used to compare salmon responses among treatments. We compared the proportion of entry events within the 2 m arena (including the contact zone) to the total events within the whole arena (4 m and 2 m arenas). We categorized length of time that salmon spent in each arena as short (< 10 s) or long (> 10 s). As the trials were carried out on multiple days, we used days as a random factor in the model. We used post-hoc Tukey tests to identify significant differences in the proportion of inner arena entries between treatments. We also compared the proportion of salmon abrupt evasive behaviours towards black and white models using ANOVA with Kruskal–Wallis (K–W)

non-parametric tests. For analyses of CNR on digital images among model-configurations, we used *t*-tests. For analyses of spatial autocorrelation coefficients, we used ANOVA but due to skew on some of the frequency distributions of autocorrelation coefficients, we also categorized the coefficients and compared different configurations with contingency tests. All statistics were performed using SPSS v24/25 (IBM).

DATA AVAILABILITY

All data on salmon responses and spectral measurements are available from the corresponding author on reasonable request.

RESULTS

We conducted 91 trials with seven model configurations during which 1617 salmon moved through the arenas. The proportion of salmon entering the inner arena for each configuration is shown in Figure 2. The highest entry rates occurred in the two controls (arena without a frame and frame, OO); however, there was a 38% reduction with OB (no body, black legs) and a 23% reduction with OW (no body, white legs) (Tukey between models: $P = 0.7$). The model with a body but no legs showed a 65% reduction relative to the control for BO but a 28% reduction for WO (Tukey between models:

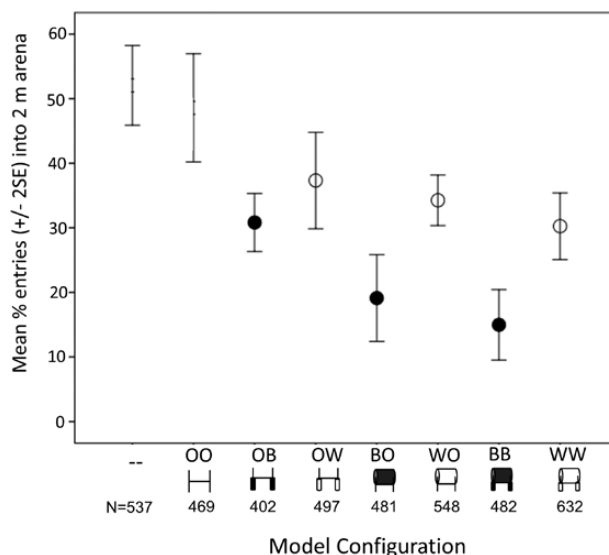


Figure 2. Mean proportions of chum salmon entry events within the inner arena to different model configurations. Error bars represent 95% confidence intervals. N = number of trials. --: no frame; OO: frame; OB: no body, black legs; OW: no body, white legs; BO: black body, no legs; WO: white body, no legs; BB: black body, black legs; WW: white body, white legs.

$P < 0.001$). Inclusion of body and legs reduced the entries from the control by 78% for BB and by 40% for WW configurations (Tukey between models: $P = 0.003$).

Abrupt evasive responses of the salmon to model configurations differed, but this varied with respect to distance (Fig. 3). There were no evasions to the frame for either the 4 m or 2 m arenas. Of the 1089 entries into the 4 m arena with black configurations (BO, OB, BB), there were 108 (9.9%) evasions, the effects of the body (BO) being approximately ten times that of legs (OB). In contrast, of the 1137 entries with white configurations (WO, OW, WW), there were two (0.2%) evasions (Fisher's exact test: $P < 0.001$). For the 2 m arena, there were 276 entries with black configurations, of which 105 (38%) were evasions whereas among 540 entries with white configurations, 90 (17%) were evasions ($K-W = 30.4$, d.f. = 5, $P < 0.001$). Similar to trends in the 4 m arena, the body-only models (BO, WO) had about ten times the evasive effect as the legs-only model (OB, OW), which were marginally more common to black legs than to white legs ($K-W = 3.8$, d.f. = 1, $P < 0.06$).

We quantified the amount of visual contrast of the above-surface models (body only) against the background through Snell's window. Through a flat-water surface and using a sub-surface camera at a depth equivalent to that of a migrating salmon and with the camera orientated towards the sky, we observed the expected differences in the CNR values between body models based on coat colour, sky or forest background (Fig. 4A-B) and camera distance. From 4 m, the

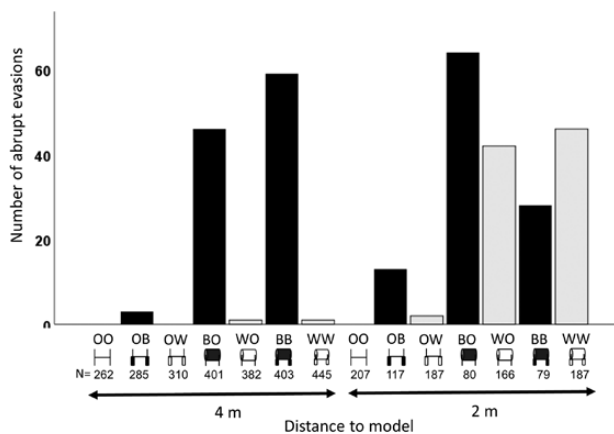


Figure 3. Mean number of abrupt evasive responses of salmon towards the different model configurations at outer (4 m) and inner (2 m + contact zone) arenas. Error bars represent 95% confidence intervals. N shows number of individual salmon entries for each configuration. OO: frame; OB: no body, black legs; OW: no body, white legs; BO: black body, no legs; WO: white body, no legs; BB: black body, black legs; WW: white body, white legs. Note that the major difference between the configurations occurs at the 4 m distance.

above-surface models were evident only at the edge of the optical window and the CNR between body colour configurations were independent of background (Sky: black $\bar{x} = 0.03 \pm 0.01$, $n = 10$; white $\bar{x} = 0.03 \pm 0.01$, $n = 10$, $t_{18} = 0.71$, $P = 0.49$; Forest: black $\bar{x} = 0.48 \pm 0.08$, $n = 10$; white $\bar{x} = 0.49 \pm 0.07$, $n = 10$, $t_{18} = 0.31$, $P = 0.76$) (t_{18} denotes t statistic with degrees of freedom for the comparison). From 2 m (Fig. 4C-F), the above-surface models projected at a higher angle in the optical window with the black model having a higher CNR than the white model against the sky background (black $\bar{x} = 0.03 \pm 0.01$, $n = 10$; white $\bar{x} = 0.03 \pm 0.01$, $n = 10$, $t_{18} = 0.16$, $P = 0.88$) but a lower CNR against the forest background (black $\bar{x} = 0.66 \pm 0.09$, $n = 10$; white $\bar{x} = 0.87 \pm 0.09$, $n = 10$, $t_{18} = 4.98$, $P < 0.001$).

We quantified the sub-surface CNR of digital images for black and white legs at 4 m, 3 m, 2 m and 1 m from the camera (Fig. 5a). Although 4 m was the approximate limit of visual detection in these water conditions, at each distance, the white legs exhibited approximately three times the contrast to the background than do black legs (Fig. 5b). However, salmon were more evasive to the black legs than the white legs, contrary to our initial prediction.

We also obtained video sequences of the models through Snell's window when influenced by natural surface waves of stream flow. Rather than a sharp delineation of the 97° optical window with a flat water surface, there was expansion up to 180° and major fragmentation of the above-surface hemisphere, including fragments of the sky projecting to the edges of the window and fragments of the models and forest background projecting into higher angles of the image (Fig. 4G-J). Through this window, the models (BO, WO) appeared as black or white fragments that shifted in position and size amid an equally shifting fragmented sky and forest background. The effects of moving surface waves, accentuated by surface ripples, was to largely eliminate the profile and integrity of the models compared to the flat surface where the intact models matched or contrasted with the forest/sky spectral background. Visual examination of individual stop frames from each video sequence also failed to resolve the integrity of model profiles although on occasional frames, larger fragments could resemble the models. This was also evident in plots of mean spatial autocorrelation coefficients which show oscillations of two orders of magnitude over sequential frames (Fig. 4K-L) but with no statistical trends for either model colour or spectral background ($F_{1,799} = 0.39$, $P = 0.53$).

DISCUSSION

Although aquatic and terrestrial habitats each have a rich history in studies of animal coloration

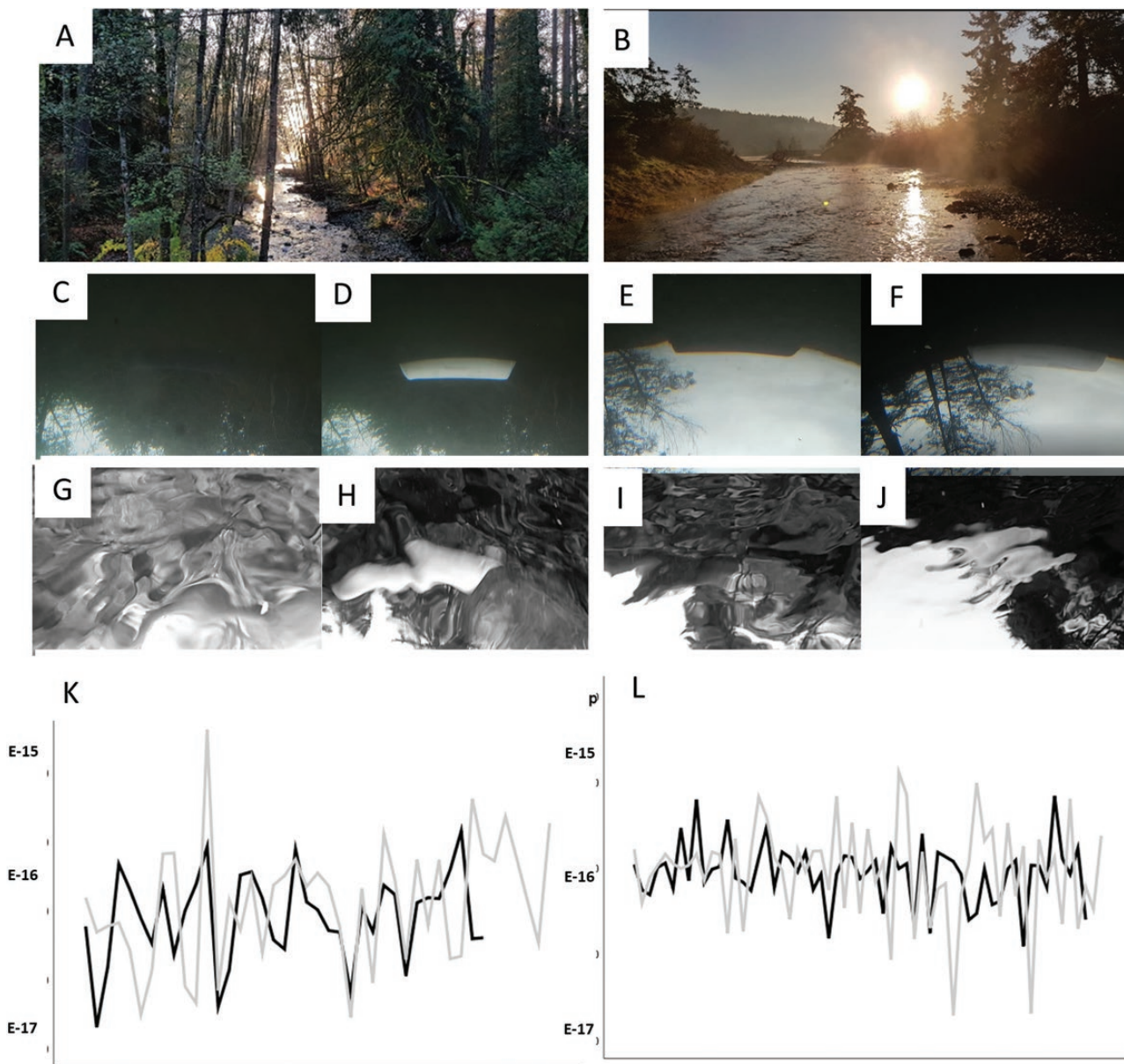
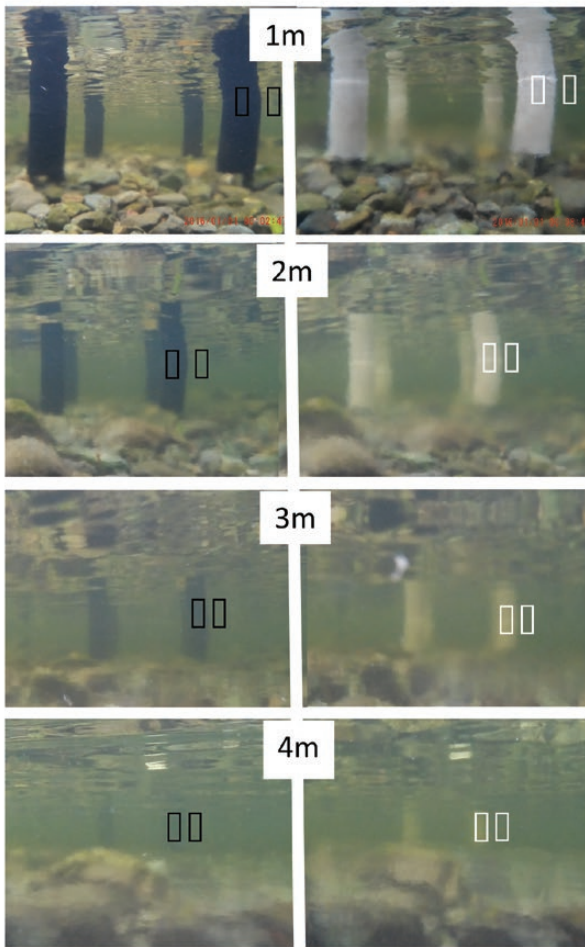


Figure 4. Representative images for study site and model configurations. A, Ayum Creek – upstream showing forest canopy. B, Ayum Creek – downstream showing open canopy. C–F, images of models through Snell’s window for a flat-water surface: (C) black model against forest background, (D) white model against forest background, (E) black model against forest/sky background, (F) white model against forest/sky background. G–J, images of models through Snell’s window for a wavy surface: (G) black model against a forest-sky background, (H) white model against a forest-sky background, (I) black model against a sky-forest background, (J) white model against a sky-forest background. K, spatial autocorrelation coefficients on sequential video frames for black model (black line) and white model (grey line) against a forest background. L, spatial autocorrelation coefficients on sequential video frames for black model (black line) and white model (grey line) against a sky-forest background.

(Cott, 1940; Lythgoe, 1979; Endler & Mappes, 2017; Caro & Mallarino, 2020), the interface between these habitats has received limited attention. We tested the hypothesis developed in Klinka & Reimchen (2009b) that the reduced avoidance of Pacific salmon to the white Kermode bear in comparison

to the black morph was due to the low spectral contrast of the white pelage against skylight as viewed through the optical window at the water-air interface. This hypothesis emerged from two major field observations: (1) the white morph had higher salmon capture success than the black morph during

A:



B

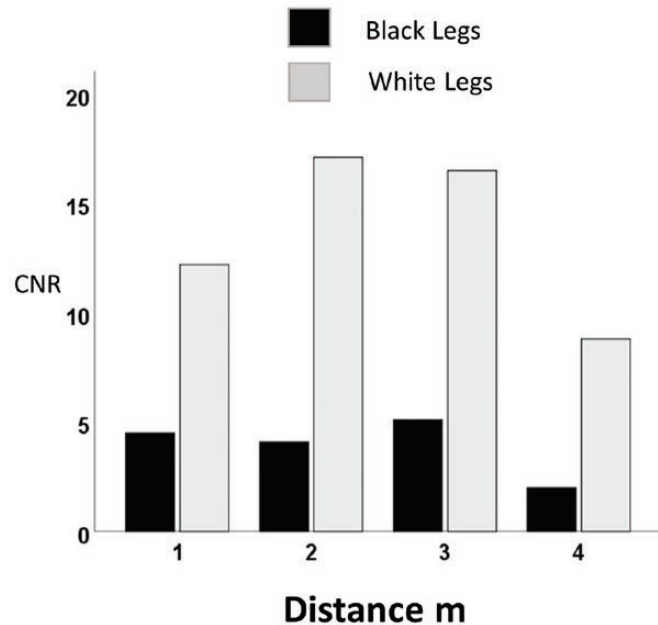


Figure 5. Sub-surface images and contrast-to-noise ratio (CNR). A, sub-surface images of model legs at four distances. B, CNR of legs for black and white legs relative to adjacent backwelling spectra. CNR data extracted from adjacent rectangles for each figure.

daylight but not during darkness; and (2) salmon were less evasive to a standing white-coated human ‘simulated predator’ than to a black-coated one during daylight but not during darkness. Subsequent studies using stable isotope analysis of hair shafts from the two morphs confirmed greater consumption of salmon by the white morph (Reimchen & Klinka, 2017). These cumulative data were consistent with the adaptive variation and multi-niche models for the maintenance of polymorphism and differed from the alternative hypothesis focusing on founder effects and geographical isolation (Hedrick & Ritland, 2011).

We placed a life-sized bear model in a stream and observed that migrating salmon avoided the black model more than the white model, passing at a greater distance and showing abrupt evasive responses in proximity to the model. Positioning a stationary model in the middle of the stream is

ecologically realistic as this ‘standing’ technique is the most common stream foraging method used by both black bears and grizzly bears (Reimchen, 1998; Klinka & Reimchen, 2002, 2009a, b). We used modular components on an aluminum frame that allowed us to independently alter below-surface (legs) and above-surface (body) effects for each coat colour. Although both the geographical location and the field protocol differed [i.e. human observers clothed in white or black overalls or a simulated bear model with white or black fleece (current study)], our results are consistent with Klinka & Reimchen (2009b), since in both studies, salmon avoided the black model at about twice the frequency of the white model, suggesting a robust response of salmon to these simulated predators. For a sub-surface observer beneath a flat-water interface, much of the above-surface horizon-to-horizon visual field is refracted into a 97° optical cone (Snell’s

window) (Horváth & Varjú, 1995). Through this cone, birds in flight would be viewed against a background of skylight; this is thought to contribute to the evolution of camouflage for the white ventral plumage found in some piscivores such as gulls (Laridae) and terns (Sternidae) (Craik, 1944; Mock, 1980; Gotmark, 1987). The expanse of skylight in the cone is narrowed in coastal marine habitats or in freshwater due to the presence of terrestrial vegetation and landforms that project into the edges of the optical window. Consequently, the sky or terrestrial background against which an above-surface predator will be viewed is dependent on their angular position from the edge of the cone. White plumage morphs of herons and egrets forage more extensively in open aquatic habitats where the background is largely sky whereas those with darker plumage tend to forage where there is more shoreline vegetation, in other words, where the piscivores are viewed against a darker background at the edge of the optical window (e.g. Murton, 1971; Mock, 1980; Caldwell, 1986; Green & Leberg, 2005; Merilaita *et al.*, 2017). We quantified the visual contrast of bear models against a sky or forest background and observed that for a flat water surface, the models at 4 m distance were detectable only at the very edge of the window and did not differ significantly in contrast as a function of background or model colour. At closer proximity (2 m) however, the models projected at a higher angle into the window and showed the predicted difference in contrast dependent on the background (forest vs. sky) and coat colour (black vs. white). This will account for the greater responsiveness of salmon with close proximity to the models.

Compared with a flat water surface, waves or ripples greatly modify the above-surface visual field through Snell's window. One component of this modification is that with increased wave angle and breaking waves, the window can expand and approach 180° allowing a sub-surface observer to see through the interface even in a horizontal plane. A second component is the concomitant fragmentation of the above-surface object, where segments near the edge of the window intrude to higher angles in the window (Lynch, 2015). Possible implications of such surface waves for predator-prey interactions have recently been examined for sub-surface photic environments (Matchette *et al.*, 2020); however, this has not been previously addressed for above-surface effects. Our videos taken through Snell's window demonstrated that the above-surface models and spectral backgrounds (sky and forest) were extensively fragmented and continuously shifting in shape and position from the continued movement of waves and ripples in the stream such that the profiles of the models could rarely be resolved. We

detected no statistical differences in mean values for any combinations of model colour (black/white) and background spectra (sky/forest, upstream/downstream). Individual stop-frames occasionally showed large fragments comprising larger proportions of a model; this was indicated by the higher spatial autocorrelation coefficients of the frame. Detection of micro-temporal shapes by salmon is reasonable, as flicker-fusion rates in fishes are comparable to terrestrial vertebrates (Horodysky *et al.*, 2010) and fish would be capable of discerning such information in the rapidly shifting visual fields. In addition, the ability to visualize a full shape from partial shapes, 'amodal completion', is deeply rooted in the evolution of vertebrates, including fishes (Sovrano & Bisazza, 2008; Truppa *et al.*, 2010) and certainly represents an adaptive behavioural response to relevant but partially occluded stimuli. The highly functional evasiveness of salmon to black fragments in the stream that dynamically vary in size, position and contrast may comprise such 'amodal completion' and recognition of their dominant predator. That the salmon in a current-dominated stream showed similar evasive responses to an upright-cloaked human observer (Klinka & Reimchen, 2009b) also suggests that moving black shapes, independent of their profile, may be a sufficient stimulus for evasive responses.

For a bear or other predator wading in a shallow stream, the legs are potentially as informative to sub-surface prey as the above-surface body. We found that salmon responses to legs-only configurations were about one-tenth of those of body-only configurations. Although this suggests that above-surface shapes are more informative to the fish, differential responsiveness may simply be due to signal strength associated with distance-related attenuation of visual signals in water. For a salmon at 20 cm depth, the above-surface model that is 400 cm horizontal distance is viewed through 20 cm of water, while the sub-surface legs are viewed through 400 cm of water. When we evaluated the relative spectral contrast for light and dark sub-surface shapes (i.e. legs), we found that white legs were approximately three times more contrasting than black legs when viewed against the stream backgrounds. Because of progressive light attenuation with distance in aquatic habitats, backwelling spectra are typically darker than the shorter path lengths of downwelling spectra and consequently, light-coloured shapes are more visible against the backwelling spectra than dark shapes (Lythgoe, 1979). This effect may have relevance to leg colour in herons and egrets (Ardeidae) as life history data from *Birds of the World* (Winkler *et al.*, 2020) indicate that in large-bodied ardeids, including those with all-white plumage, leg colour is usually very dark, as would be predicted for

background matching and camouflage against fish prey. Small-bodied ardeids such as the white cattle egret (*Bubulcus ibis*) have pale-coloured legs and are commonly associated with foraging in terrestrial rather than aquatic habitats.

We predicted that salmon would exhibit greater avoidance to sub-surface white legs due to their greater contrast against the dark horizontal background but contrary to our prediction, salmon were marginally more evasive to black legs. This might indicate that the corresponding increased evasiveness to the above-surface black model is due to avoidance of black shapes rather than the camouflage of the white model. Black bears are dominant predators on salmon in the majority of streams and rivers entering the north-east Pacific, including the current study stream. These predator-prey interactions allow multiple exposure and learned avoidance responses of the salmon to foraging bears. Such interactions have continuity back to the late Pliocene when *Ursus* emerged (Talbot & Shields, 1996; Luna-Arangur *et al.*, 2020) and could have favoured an adaptive behavioural predisposition in salmon for increased avoidance of shapes associated with this predator. Because the high salmon capture rate that bears exhibit, often at low light levels (Reimchen, 1998, 2000; Klinka & Reimchen, 2002, 2009a) and predominantly in turbulent streams, implies high fitness benefit to salmon that respond rapidly. This may be equivalent to previous evidence that salmon have an innate behavioural avoidance to weak concentrations of chemical extracts from tissues extracted from bears (Brett & MacKinnon, 1954).

Our new data strongly support the original study (Klinka & Reimchen, 2009b) that salmon are less evasive to white models than dark models. However, the data also suggest that coat colour background matching may not be the only mechanism for the salmon responses. The accentuated evasion of the salmon to black shapes, even in sub-surface conditions where the black configuration is less conspicuous than the white model may reflect a heritable predisposition to avoid dark shapes rather than a contrast reduction of a white morph against skylight. However, given the relatively well-recognized foraging advantage of white plumage in some avian piscivores (Green & Leberg, 2005), a combination of these processes may be operating for the Kermode bear. In broader context, the dynamic fragmentation of the visual field through the water-air interface identified in this study will vary among habitats differing in current, wind and background and could be expected to influence spatial and temporal choices in foraging times as well as the nature of adaptive coat or plumage coloration.

ACKNOWLEDGEMENTS

We thank Martin Lechowicz for suggesting Ayum Creek, and Michael Clinchy, Don Kramer, Larry Dill and Peter Abrams for discussion. John Taylor assisted with spectral measurements of the models and Sheila Douglas provided comments on the manuscript. The research was supported by an Natural Sciences and Engineering Research Council of Canada (NSERC) operating grant to T.E.R. (NRC2354). This work was carried out on the traditional lands of the T'Sou-ke peoples, we declare no conflict of interests. T.E.R. developed the study and designed the field experiments and was primarily responsible for writing the manuscript. D.H. and J.H.E. undertook the experiments, D.H. and T.E.R. performed the underwater imagery. D.H., J.H.E. and T.E.R. were each involved in statistical analyses of the data. All authors read and approved the final draft.

REFERENCES

- Beaudet L, Novales Flamarique I, Hawryshyn CW. 1997. Cone photoreceptor topography in the retina of sexually mature Pacific salmonid fishes. *Journal of Comparative Neurology* **383**: 49–59.
- Brett JR, MacKinnon D. 1954. Some aspects of olfactory perception in migrating adult coho and spring salmon. *Journal of the Fisheries Research Board of Canada* **11**: 310–318.
- Byun SA, Koop B, Reimchen TE. 1997. North American black bear mtDNA phylogeography: implications for morphology and the Haida Gwaii refugium controversy. *Evolution* **51**: 1647–1653.
- Caldwell GS. 1986. Predation as a selective force on foraging herons - effects of plumage color and flocking. *Auk* **103**: 494–505.
- Carleton KL, Escobar-Camacho D, Stieb SM, Cortesi F, Marshall NJ. 2020. Seeing the rainbow: mechanisms underlying spectral sensitivity in teleost fishes. *Journal of Experimental Biology* **223**: jeb193334.
- Caro T, Mallarino R. 2020. Coloration in mammals. *Trends in Ecology and Evolution* **35**: 357–366.
- Cott H. 1940. *Adaptive coloration in animals*. London: Methuen.
- Cowan IM, Guiguet CJ. 1956. *The mammals of British Columbia*. Victoria: Provincial Museum of Natural History and Anthropology.
- Craik KJW. 1944. White plumage in sea-birds. *Nature* **153**: 288.
- Day RD, Mueller F, Carseldine L, Meyers-Cherry N, Tibbitts IR. 2016. Ballistic Beloniformes attacking through Snell's window. *Journal of Fish Biology* **88**: 727–734.
- Endler JA, Mappes J. 2017. The current and future state of animal coloration research. *Philosophical Transactions of the Royal Society B: Biological Sciences* **372**: 20160352.

- Ford EB. 1964.** *Ecological genetics*. London: Methuen.
- Gotmark F. 1987.** White underparts in gulls function as hunting camouflage. *Animal Behaviour* **35**:1786–1792.
- Green MC, Leberg PL. 2005.** Influence of plumage color on prey response: does habitat alter heron crypsis to prey? *Animal Behaviour* **70**: 1203–1208.
- Hailman JP. 1977.** *Optical signals*. London: Indiana University Press.
- Hedrick PW, Ritland L. 2011.** Population genetics of the white-phased “Spirit” black bear of British Columbia. *Evolution* **66**: 305–313.
- Horodysky AZ, Brill RW, Warrant EJ, Musick JA, Latour RJ. 2010.** Comparative visual function in four piscivorous fishes inhabiting Chesapeake Bay. *Journal of Experimental Biology* **213**: 1751–1761.
- Horváth G, Varjú D. 1995.** Underwater refraction-polarization patterns of skylight perceived by aquatic animals through Snell’s window of the flat water surface. *Vision Research* **35**: 1651–1666.
- Klinka DR, Reimchen TE. 2002.** Nocturnal and diurnal foraging behaviour of brown bears (*Ursus arctos*) on a salmon stream in coastal British Columbia. *Canadian Journal of Zoology* **80**: 1317–1322.
- Klinka DR, Reimchen TE. 2009a.** Darkness, twilight, and daylight foraging success of bears (*Ursus americanus*) on salmon in coastal British Columbia. *Journal of Mammalogy* **90**: 144–149.
- Klinka DR, Reimchen TE. 2009b.** Adaptive coat color polymorphism in the Kermode bear of coastal British Columbia. *Biological Journal of the Linnean Society* **98**: 479–488.
- Luna-Arangur C, Soberon J, Vazquez-Dominguez E. 2020.** A tale of four bears: environmental signal on the phylogeographical patterns within the extant *Ursus* species. *Journal of Biogeography* **47**: 472–486.
- Lynch DK. 2015.** Snell’s window in wavy water. *Applied Optics* **54**: B8–B11.
- Lythgoe JN. 1979.** *The ecology of vision*. Oxford: Clarendon.
- Marshall HD, Ritland M. 2002.** Genetic diversity and differentiation of Kermode bear populations. *Molecular Ecology* **11**: 685–697.
- Matchette SR, Cuthill IC, Cheney KL, Marshall NJ, Scott-Samuel NE. 2020.** Underwater caustics disrupt prey detection by a reef fish. *Proceedings of the Royal Society of London B* **287**: 20192453.
- Merilaita S, Scott-Samuel NE, Cuthill IC. 2017.** How camouflage works. *Philosophical Transactions of the Royal Society of London B: Biological Sciences* **372**: 20160341.
- Mock DW. 1980.** White-dark polymorphism in herons. *Proceedings of the First Welder Wildlife Foundation Symposium* **1**: 145–161.
- Murton RK. 1971.** Polymorphism in Ardeidae. *Ibis* **113**: 97–98.
- Reimchen TE. 1998.** Nocturnal foraging behaviour of black bear, *Ursus americanus*, on Moresby Island, British Columbia. *Canadian Field Naturalist* **112**: 446–450.
- Reimchen TE. 2000.** Some ecological and evolutionary aspects of bear-salmon interactions in coastal British Columbia. *Canadian Journal of Zoology* **78**: 448–457.
- Reimchen TE, Klinka DR. 2017.** Niche differentiation between coat color morphs in the Kermode bear (Ursidae) of coastal British Columbia. *Biological Journal of the Linnean Society* **122**: 274–285.
- Ritland K, Newton C, Marshall HD. 2001.** Inheritance and population structure of the white-phased “Kermode” black bear. *Current Biology* **11**: 1468–1472.
- Service CN, Bourbonnais M, Adams MS, Henson L, Neasloss D, Picard C, Paquet PC, Darimont CT. 2020.** Spatial patterns and rarity of the white-phased ‘Spirit bear’ allele reveal gaps in habitat protection. *Ecological Solutions and Evidence* **1**: e12014.
- Sovrano VA, Bisazza A. 2008.** Recognition of partly occluded objects by fish. *Animal Cognition* **11**: 161–166.
- Talbot SL, Shields GF. 1996.** Phylogeny of the bears (Ursidae) inferred from complete sequences of three mitochondrial genes. *Molecular Phylogenetics and Evolution* **3**: 567–575.
- Truppa V, Sovrano VA, Spinozzi G, Bisazza A. 2010.** Processing of visual hierarchical stimuli by fish (*Xenotoca eiseni*). *Behavioural Brain Research* **207**: 51–60.
- Ursell T. 2020.** *autocorr2d*. MATLAB Central File Exchange. Available at: <https://www.mathworks.com/matlabcentral/fileexchange/67348-autocorr2d>. Accessed 13 September 2020.
- Winkler DW, Billerman SM, Lovette IJ. 2020.** In: Billerman SM, Keeney BK, Rodewald PG, Schulenberg TS, eds. *Herons, egrets, and bitterns (Ardeidae), version 1.0. Birds of the World*. Ithaca: Cornell Lab of Ornithology.

SUPPORTING INFORMATION

Additional Supporting Information may be found in the online version of this article at the publisher’s web-site:

Video S1. Kermode bear salmon capture. Credit: Dr. J.B. Foster. Date of filming: October 2000. Locality: Canoona River, Princess Royal Island, British Columbia, Canada.